

Real-time 3D-aware Portrait Editing from a Single Image

QINGYAN BAI, The Hong Kong University of Science and Technology, China

YINGHAO XU, Stanford University, USA

ZIFAN SHI, The Hong Kong University of Science and Technology, China

HAO OUYANG, The Hong Kong University of Science and Technology, China

QIUYU WANG, Ant Group, China

CEYUAN YANG, Shanghai AI Laboratory, China

XUAN WANG, Ant Group, China

GORDON WETZSTEIN, Stanford University, USA

YUJUN SHEN*, Ant Group, China

QIFENG CHEN*, The Hong Kong University of Science and Technology, China

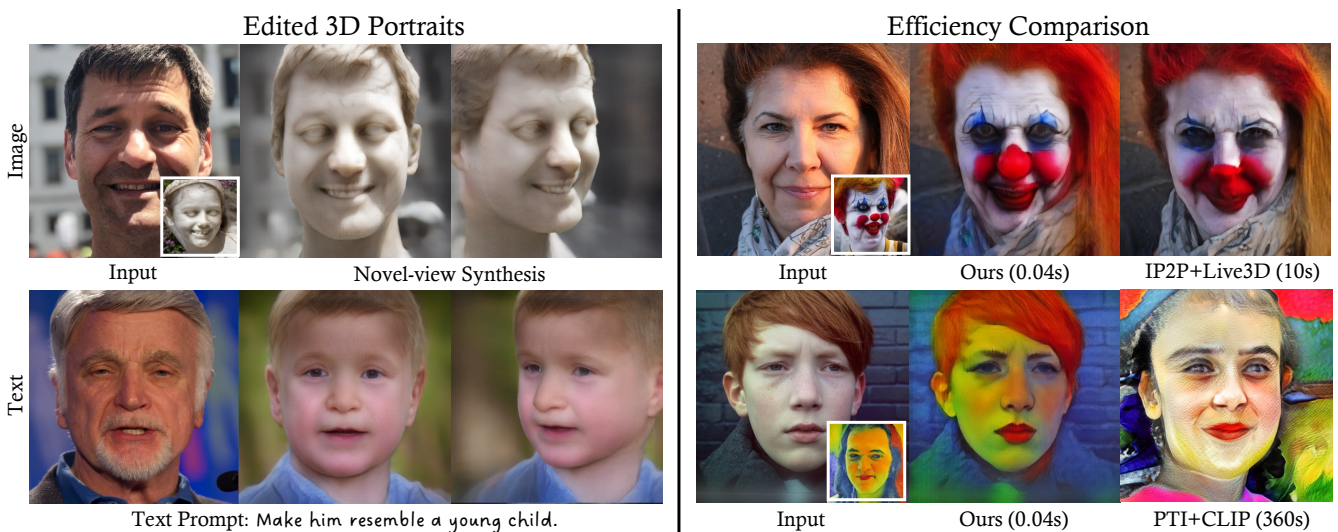


Fig. 1. **Photorealistic editing results** produced by our proposed **3DPE**, which allows users to perform 3D-aware portrait editing using image or text prompts. In comparison with baseline methods, such as InstructPix2Pix [Brooks et al. 2023]+Live3D [Trevithick et al. 2023] and PTI [Roich et al. 2022]+CLIP [Radford et al. 2021] (details are illustrated in Sec. 4), our approach accurately follows the guidance from reference prompts and maintains sufficiently better efficiency.

This work presents **3DPE**, a practical tool that can efficiently edit a face image following given prompts, like reference images or text descriptions, in the 3D-aware manner. To this end, a lightweight module is distilled from a 3D portrait generator and a text-to-image model, which provide prior knowledge of face geometry and open-vocabulary editing capability, respectively. Such a design brings two compelling advantages over existing approaches. First, our system achieves *real-time* editing with a feedforward network (*i.e.*, ~ 0.04 s per image), over 100 \times faster than the second competitor. Second, thanks to the powerful priors, our module could focus on the learning of editing-related variations, such that it manages to handle various types of editing simultaneously in the training phase and further supports *fast adaptation*

*Corresponding authors.

Authors' addresses: Qingyan Bai, The Hong Kong University of Science and Technology, China; Yinghao Xu, Stanford University, USA; Zifan Shi, The Hong Kong University of Science and Technology, China; Hao Ouyang, The Hong Kong University of Science and Technology, China; Qiuyu Wang, Ant Group, China; Ceyuan Yang, Shanghai AI Laboratory, China; Xuan Wang, Ant Group, China; Gordon Wetzstein, Stanford University, USA; Yujun Shen, Ant Group, China; Qifeng Chen, The Hong Kong University of Science and Technology, China.

to user-specified novel types of editing during inference (*e.g.*, with ~ 5 min fine-tuning per case). The code, the model, and the interface will be made publicly available to facilitate future research.

Additional Key Words and Phrases: 3D-aware portrait, efficient editing

1 INTRODUCTION

Inferring the geometry and appearance from a single-view portrait image has become mature and practical [Gao et al. 2020; Ko et al. 2023; Lin et al. 2022; Sun et al. 2022a; Trevithick et al. 2023; Wang et al. 2022; Xie et al. 2023], largely attributed to the utilization of priors in various 2D/3D generative models. However, only performing geometry reconstruction is insufficient. The significance of 3D editing of portraits, driven by user intentions, and the need for streamlined efficiency in the editing process has been steadily increasing. This is particularly crucial in real-world applications such as AR/VR, 3D telepresence, and video conferencing, where real-time editing is often essential. Consequently, a key question arises: How

can we effectively address the challenge of attaining high-fidelity portrait editing while ensuring real-time efficiency?

Traditional tools for 3D portrait editing [Deng et al. 2020] typically rely on template facial models [Blanz and Vetter 2023; Paysan et al. 2009], which has limitations in handling the substantial geometry changes because it often overlooks precise features like hair and beard. Recent 3D GANs [Chan et al. 2022, 2021; Schwarz et al. 2020; Shi et al. 2022a; Xia and Xue 2023] show remarkable capabilities in generating high-fidelity 3D portraits. They can serve as powerful generative priors for 3D portrait editing when coupled with GAN inversion techniques [Abdal et al. 2019, 2020; Shen et al. 2020b; Zhu et al. 2020, 2016]. However, these methods may encounter issues related to geometry distortion or exhibit slow speed, and the editing is constrained by the limited latent attributes. Besides, 2D diffusion models can offer a strong prior with SDS loss [Poole et al. 2022] for editing purposes [Hertz et al. 2023]. Nonetheless, they often require step-by-step optimization and become a major bottleneck for real-time applications.

To this end, we present **3DPE**, a real-time **3D-aware Portrait Editing** method driven by user-defined prompts. As shown in Fig. 1, when provided with a single-view portrait image, our approach empowers a versatile range of editing through flexible instructions, including images and text. We leverage the powerful 3D prior from a 3D-aware face generator and achieve a high-fidelity 3D reconstruction of the portrait image. Subsequently, we distill editing knowledge from an open-vocabulary text-to-image model into a lightweight module integrated with the 3D-aware generator. This module, characterized by its minimal computational cost, allows our system to maintain real-time inference and excel in handling various types of editing, all the while ensuring good 3D consistency. An additional advantage is that our model supports customization through user-specified prompts with fast adaptation speed. This empowers users to build their own editing model at a minimal cost, enabling our system to cater to a broader audience.

Our system achieves real-time 3D-aware portrait editing through the utilization of a feedforward network, with a processing time of 40ms on a standard customer GPU. Additionally, we present a comprehensive evaluation of our method using various prompts both quantitatively and qualitatively. Our design choices are also validated through comparisons with ablated variants of our method. Compared with baseline methods, our approach demonstrates superior 3D consistency, precise texture alignment, and a substantial improvement in inference time, as reflected by the evaluation metrics. We demonstrate the versatility of our method by showcasing its capacity to perform a wide variety of edits, including text and image prompts, on portrait images. The code, the model and the interface will be made publicly available.

In summary, the contributions of our work include:

- We propose a lightweight module to distill knowledge from 3D GANs and diffusion models for 3D-aware editing from a single image. Due to the minimal cost of the new module, our model maintains real-time performance.
- Our model supports fast adaptation to user-specified editing, requiring only 10 image pairs and 5 minutes for the adaptation.

- Our model can accommodate various control signals, including text and image prompts.

2 RELATED WORK

2.1 Generative Face Priors

Generative models aim at modeling the underlying distribution of the data, containing a wealth of prior knowledge. Recently, 3D GANs [Chan et al. 2022, 2021; Gu et al. 2022; Or-El et al. 2022; Pan et al. 2021; Schwarz et al. 2020, 2022; Shi et al. 2023, 2022b; Skorokhodov et al. 2022; Wang et al. 2023b; Xu et al. 2022] are mostly adopted to learn 3D faces from single-view image dataset. The interior rich domain-specific geometry priors enable various face-related applications such as image editing [Cai et al. 2022; Sun et al. 2022a,b; Trevithick et al. 2023]. Large-scale diffusion models [Rombach et al. 2022], in contrast, encode knowledge of huge datasets and thus can provide general prior information. Such priors are broadly leveraged for tasks such as image editing [Brooks et al. 2023; Cao et al. 2023; Graikos et al. 2022; Haque et al. 2023; Meng et al. 2021; Zhang et al. 2023], customization [Hu et al. 2021; Kumari et al. 2023; Liu et al. 2023a; Ruiz et al. 2023], and video editing [Ceylan et al. 2023; Chai et al. 2023; Geyer et al. 2023; Liu et al. 2023b; Ouyang et al. 2023; Qi et al. 2023; Wang et al. 2023a; Yang et al. 2023]. In our approach, we capitalize on the advantages of both the geometry prior derived from 3D GANs and the broader editing prior offered by large-scale text-to-image diffusion models, instead of relying solely on a single type of prior.

2.2 Portrait Editing from a Single Image

Although many methods work well for reconstructing [Gao et al. 2020; Guo et al. 2022] or generating [Chan et al. 2022] faces, editing has become a necessary interface to connect these methods with real-world applications. Previously, portrait editing given single-view image was mostly completed in 2D image space facilitated with GAN inversion [Abdal et al. 2019, 2020; Bai et al. 2022; Härkönen et al. 2020; Roich et al. 2022; Shen et al. 2020a,b; Xu et al. 2021; Zhu et al. 2020], which enables fast editing by exploring the trajectories in the GAN’s latent space. Recent diffusion-based portrait editing [Brooks et al. 2023; Zhang et al. 2023] can support various editing types with texts as guidance. However, most of them are done in the 2D space, and thus there is no guarantee for the underlying 3D consistency. Therefore, 3D-aware portrait editing is crucial to achieve the goal. Some methods [Chang et al. 2023; Jiang et al. 2023; Li et al. 2023a; Lin et al. 2022; Sun et al. 2022a,b; Wang et al. 2022; Xie et al. 2023; Yin et al. 2023] rely on the latent space of 3D GANs to perform editing through walking in the latent space, but are limited by the number of editable latent attributes. A few methods, such as Instruct-NeRF2NeRF [Haque et al. 2023], Clip-Face [Aneja et al. 2023], and LENeRF [Hyung et al. 2023], attempt to leverage the large-scale open-vocabulary models [Radford et al. 2021; Rombach et al. 2022] to edit on 3D representations with texts as guidance but require heavy iterative refinement of the edited results. Similarly, InstructPix2NeRF [Li et al. 2023b] leverages text-to-image models and text prompts to edit the latent space of the GAN-based 3D generator. However, it is held back by the multi-step

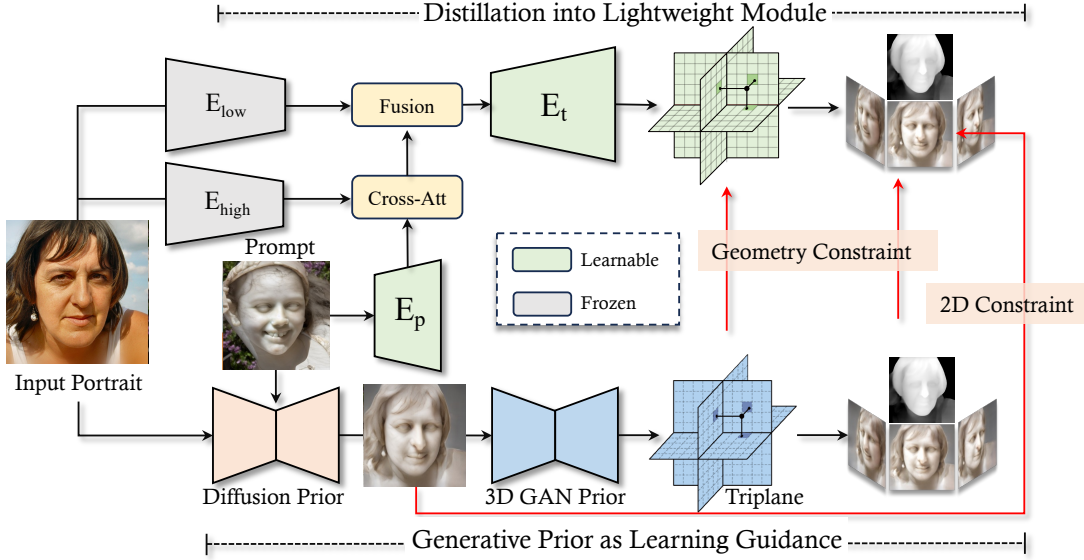


Fig. 2. **Overview of our method.** We distill the prior in the diffusion model and 3D GAN for real-time 3D-aware editing. Our approach is fine-tuned from Live3D [Trevithick et al. 2023], where we extract features from the input portrait I using $E_{high}(\cdot)$ and $E_{low}(\cdot)$. The prompt embedding is generated with $E_p(\cdot)$ and injected with the input features from $E_{high}(\cdot)$ through a cross-attention mechanism. Our model is trained to mimic the output from the diffusion prior to acquire editing knowledge and enforce geometry constraints through triplane, multi-view images, and depth supervision from the 3D prior. In this context, InstructPix2Pix [Brooks et al. 2023] and Live3D serve as the diffusion and 3D prior, respectively. It’s noteworthy that only $E_p(\cdot)$ and $E_t(\cdot)$ are learnable during training, while all other parameters remain frozen.

diffusion inference and the heavy structure of a GAN-based generator. Ours, in contrast, benefits from the lightweight design of the module and achieves real-time editing with ease. With such a design, our model can also adapt to novel editing prompts faster than previous methods. Moreover, texts cannot always illustrate the desired effects precisely, and sometimes an image prompt serves as a better guidance for image editing. Our method can support not only text prompts but also image prompts for editing, providing a more flexible and user-friendly interface.

3 METHOD

Our approach takes a portrait image I and its camera pose c , obtained via the face pose estimator [Deng et al. 2019b]. Additionally, the referenced prompts P (images or texts) serve as the editing instructions. The outcome of our model is an edited version of the 3D portraits characterized by NeRF in accordance with the prompts. The edited image is denoted as I_p . Within our framework, we achieve this objective by leveraging the knowledge of 3D GANs and an open-vocabulary text-to-image model, which is distilled into a lightweight module. Following distillation, our method enables real-time 3D portrait editing and efficient adaptation to user-specified prompts.

In Sec. 3.1, we offer an illustration of 3D GANs and diffusion models. The process of distilling these priors into a lightweight module is outlined in Sec. 3.2. Finally, the details for model training and inference, along with the fast adaptation for novel prompts, are presented in Sec. 3.3.

3.1 Preliminary

3D GAN Prior for Portrait Reconstruction. The 3D-aware GANs showcase the ability to synthesize photorealistic 3D images using a collection of single-view images. Notably, EG3D [Chan et al. 2022] introduces an efficient triplane 3D representation, demonstrating high-quality 3D-aware image rendering. Once trained, the generator of EG3D can be applied for single-image 3D reconstruction via GAN inversion. However, existing 3D GAN inversion methods often encounter geometry distortion or exhibit slow inference speed. To tackle these challenges, we utilize Live3D [Trevithick et al. 2023], a state-of-the-art single-image portrait 3D reconstruction model built upon EG3D, preserving geometry quality while ensuring real-time performance. Live3D employs a two-branch encoder, $E_{high}(\cdot)$ and $E_{low}(\cdot)$, to extract different resolution features from the input image. It then utilizes a ViT-based $E_t(\cdot)$ decoder [Dosovitskiy et al. 2020] to transform the fused encoder features into the triplane, T :

$$T = E_t(E_{high}(I), E_{low}(I)) \quad (1)$$

This triplane T is subsequently used in conjunction with the volume rendering module and upsample of EG3D to generate photorealistic view synthesis given the camera pose c . For clarification, we use $R(\cdot)$ to denote this process.

Diffusion Prior for Portrait Editing. Only performing 3D reconstruction is insufficient as our goal is to edit portrait images. Large-scale diffusion models [Rombach et al. 2022], trained on vast text-image pairs, can synthesize realistic photos with text input, offering a powerful editing prior. Despite their effectiveness for

face images, the editing process is often slow due to step-by-step optimization or multiple inferences in diffusion models. Moreover, obtaining a large amount of high-quality paired data with multi-view consistency from the diffusion model is extremely challenging, resulting in the application of 3D-aware editing from a single image impractical. Therefore, our goal is to distill editing knowledge from the diffusion model, integrate it with the 3D prior in Live3D into a lightweight module, and employ it for real-time portrait editing.

3.2 Distilling Priors into a Lightweight Module

Our system aims to perform real-time 3D-aware editing for various prompts for the single-view portrait. Thus, it needs powerful 3D knowledge for geometry reconstruction and editing prior to handling various control signals. We leverage the strengths of both 3D GANs and diffusion models. In the following, we provide detailed presentations on how the knowledge of these two types of models is distilled into a lightweight module.

Feature Representation in Live3D. We carefully study the Live3D model and discover that, as a two-branch triplane-based 3D reconstruction model, the low-resolution and high-resolution features from the Live3D encoder $E_{low}(\cdot)$ and $E_{high}(\cdot)$ tend to learn various levels of information without explicit guidance. We conduct a study by disabling one of the branches and inferring the reconstructed images. As illustrated in Fig. 3, when the high-resolution encoder $E_{high}(\cdot)$ is disabled, the inference image retains a similar structure but loses its detailed appearance. Conversely, when the low-resolution encoder $E_{low}(\cdot)$ is disabled, the reconstructed portraits preserve some of the texture from the input but struggle to capture the geometry. Based on this analysis, the features of the two branches separately model low-frequency and high-frequency information. This insight motivates our model design in terms of how to distill knowledge from the diffusion model and 3D GANs.

Geometry Prediction for Inputs I. In our framework, we use the prompts P to refine the input portrait I into the edited image I_p . The I_p inherits a similar structure to the input I , providing coarse geometry or structural guidance in the editing process. As discussed in the above section, the encoder $E_{low}(\cdot)$ consistently generates low-frequency features to represent geometry cues, making it well-suited for preserving structured information in the input portrait. As a result, we freeze $E_{low}(\cdot)$ and leverage it to produce structure features $F_g = E_{low}(I)$ for coarse geometry prediction.

Injecting Prompts P as Condition. In contrast to input images, prompts typically offer more high-frequency and texture information to guide and control the editing process. Accordingly, it is appropriate to incorporate the prompts into the high-level branch $E_{high}(\cdot)$ in Live3D to extract the high-frequency features. To incorporate prompts, we utilize the prompt encoder $E_p(\cdot)$ to create prompt embeddings that are fused into our model through cross attention, which is similar to the strategy in Stable Diffusion [Rombach et al. 2022]. Specifically, we add a cross-attention layer after $E_{high}(\cdot)$ to obtain the feature updated with the prompt embeddings:

$$F_a = \text{crossatt}(E_{high}(I), E_p(P)), \quad (2)$$

where the encoder $E_p(\cdot)$ is a transformer (MAE [He et al. 2022] for image and CLIP [Radford et al. 2021] for text). The $E_{high}(I)$

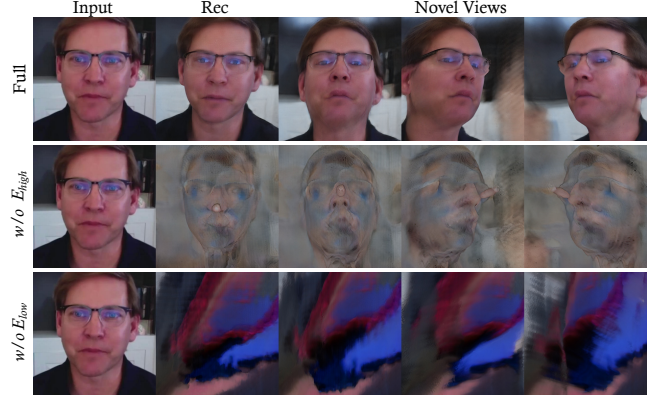


Fig. 3. **Disentanglement in Live3D features.** We separately disable the features from $E_{high}(\cdot)$ and $E_{low}(\cdot)$ to infer the reconstructed image. Without $E_{high}(\cdot)$, the output retains the coarse structure but loses the appearance. Conversely, when $E_{low}(\cdot)$ is deactivated, the reconstructed portraits preserve the texture (such as the blue and purple reflection on the glasses) but fail to capture the geometry.

serves as the query and $E_p(P)$ is employed as key and value. The updated feature F_a and the geometry feature F_g are then feed into the decoder $E_t(\cdot)$ to infer the triplane T_p :

$$T_p = E_t(F_a, F_g). \quad (3)$$

Distilling Diffusion and 3D GAN Prior. Unlike previous methods that require large amounts of 3D data, our model operates with only 2D paired data generated by the 2D editing model [Brooks et al. 2023] during training. For visual prompts, we perform captioning [Li et al. 2022] on P and then use the captions as the instruction to generate an edited image I_{gt} with 2D diffusion model [Brooks et al. 2023] as the pseudo label. For text prompts, we follow a similar process but skip the captioning step. With the predicted triplane T_p , we can render the image using the pretrained EG3D model and then calculate the reconstruction loss as follows:

$$\mathcal{L}_{2d} = \ell_1(I_{gt}, R(T_p, c)), \quad (4)$$

where $R(\cdot)$ is the rendering module of EG3D, c is the camera pose of input portrait, and $\ell_1(\cdot)$ is an image reconstruction loss penalizing the difference between the ground truth I_{gt} and the rendering $I_p = R(T_p, c)$. It's important to note that \mathcal{L}_{2d} , used to reconstruct the I_{gt} , essentially distill the knowledge of editing from the diffusion model.

We observe that \mathcal{L}_{2d} helps the model to reconstruct well on the input camera view but suffers from geometry distortion during novel-view synthesis. To fully exploit the 3D properties of Live3D, we propose to distill the 3D knowledge of Live3D. Specifically, we leverage the pretrained Live3D to infer the triplane T_{gt} , and multi-view depths \mathcal{D}_{gt} and images I_{gt} of the pseudo-label image I_{gt} :

$$T_{gt}, \mathcal{D}_{gt} = G(I_{gt}, C), \quad (5)$$

where $G(\cdot)$ represents the inference process of Live3D, where $C = \{c_1, \dots, c_n\}$ is the camera set, and n denotes the number of cameras. We also render the multi-view depths \mathcal{D}_p and images I_p of the

edited image I_p from the triplane T_p and then define the objective:

$$\mathcal{L}_{3d} = \ell_I(I_p, I_{gt}) + \ell_T(T_p, T_{gt}) + \ell_D(D_p, D_{gt}), \quad (6)$$

where $\ell_I(\cdot)$, $\ell_T(\cdot)$ and $\ell_D(\cdot)$ is the reconstruction loss penalizing the difference in image, triplane, and depth between I_p and I_{gt} .

3.3 Training and Inference

Training. During the training phase, we sample a triplet consisting of the input portrait I along with its camera pose c , prompts P , and the pseudo-label image I_{gt} generated by the 2D diffusion model. We leverage the Live3D model as a pretrained model and add an additional prompts encoder E_p to extract prompts embeddings. The overall learning objective can be described as follows:

$$L = \lambda_1 L_{2D} + \lambda_2 L_{3D}, \quad (7)$$

where λ_1 and λ_2 are loss weights. In our setting, λ_1 and λ_2 are both set to 1.0. For the reconstruction loss, $\ell_I(\cdot)$, $\ell_T(\cdot)$ are combinations of L_2 loss and LPIPS loss [Zhang et al. 2018], with loss weights being 1 and 2, respectively. $\ell_D(\cdot)$ and $\ell_T(\cdot)$ are L_1 loss. Notably, during training, only $E_p(\cdot)$, $E_t(\cdot)$ are learnable, while other modules are frozen. It allows our model to leverage Live3D knowledge as much as possible and converge at a very fast speed.

Inference. For inference, users can provide a single portrait image and choose prompts used during our training. Our model is able to generate the edited 3D NeRF along with photorealistic view synthesis.

Customized Prompts Adaptation. To accommodate customized styles provided by users, we propose a method to adapt our pretrained encoder to novel prompts. We increase the tuning efficiency by optimizing only $E_p(\cdot)$ and the normalization layers in $E_t(\cdot)$ with the same learning objective Eq. 7. This method allows us to limit the training data to only 10 image pairs and the learning time to 5 minutes on a single GPU.

4 EXPERIMENTS

4.1 Experimental Setup

Training Settings. For real faces, we adopt the FFHQ dataset [Karras et al. 2019] at 512×512 resolution with camera parameters aligned by EG3D [Chan et al. 2022]. In order to obtain the stylized images as pseudo labels and visual prompts, we leverage InstructPix2Pix [Brooks et al. 2023] to edit the real faces. Specifically, given an image prompt, we first employ BLIP [Li et al. 2022] for captioning and use the obtained text as the instruction to synthesize an edited image with InstructPix2Pix. We totally conduct experiments on 20 styles, and for each style, we synthesize 1000 images, resulting in 20,000 image pairs for model training. For each style, we use 8 textual prompts for training and 5 textual prompts for testing. We adopt a learning rate of $5e-5$ and optimize the model for 60k iterations with a batch size of 32. The entire training procedure is completed over a period of 40 hours utilizing 8 NVIDIA A100 GPUs.

Baselines. We conduct comparisons against two categories of methods that achieve analogous outcomes: 1) 3D construction coupled with 3D editing; 2) 2D editing followed by 3D reconstruction. For the first category, we implement two baseline approaches, wherein we leverage PTI [Roich et al. 2022] or Live3D [Trevithick et al. 2023]

Table 1. Quantitative comparisons. We compare several baselines on the 100 images of FFHQ dataset. It’s important to note that we exclude CLIP, for PTI+CLIP and Live3D+CLIP since these models utilize CLIP for optimization. Our model excels in 3D quality and achieves a remarkable 250x improvement (compared with IP2P+Live3D) in inference speed, achieving real-time performance.

Method	$ID_t \uparrow$	$CLIP_r \uparrow$	$3D \uparrow$	Time \downarrow
PTI+CLIP	0.11	-	0.73	360s
Live3D+CLIP	0.63	-	0.72	30s
IP2P+Live3D	0.52	0.59	0.75	10s
Ours	0.47	0.73	0.76	0.04s

for reconstruction and augment both of them with CLIP loss [Radford et al. 2021] for editing. In the second category, we employ an instructive pixel-to-pixel editing method [Brooks et al. 2023] prior to executing 3D reconstruction via Live3D.

Evaluation Criteria. We evaluate all metrics on 100 pairs of images processed from FFHQ. We conduct a comprehensive evaluation of the editing performance in the following four aspects: identity preservation, reference alignment, 3D consistency, and inference speed. 1) **Identity preservation (ID_t)** aims to measure the preservation of the original identity by calculating the cosine similarity between the identity feature of the input image I and that of the edited image I_p . We use ArcFace model [Deng et al. 2019a] to extract identity features. 2) **Reference alignment ($CLIP_r$)** targets at assessing the alignment of the output editing styles to the desired input prompt by computing the cosine similarity in the CLIP [Radford et al. 2021] feature space. 3) **3D consistency (3D)** on the edited outputs is measured following the evaluation protocols established by EG3D [Chan et al. 2022]. This involves calculating the identity similarity across multiple views. 4) **Inference speed (Time)** is measured on a single NVIDIA A6000 GPU with an average of 100 samples.

4.2 Efficient 3D-aware Portrait Editing

We make in-depth analysis of our efficient portrait editing system both quantitatively and qualitatively. The results are included in Tab. 1 and Fig. 4. For reference alignment, we do not report $CLIP_r$ for methods that leverage CLIP for optimization since it is evaluated with CLIP as well. The standout feature of our system is its efficiency. Our method achieves an inference speed of merely 40ms, which improves over 100 times compared to the fastest existing baselines, which require around 10 seconds. Because of the efficient knowledge distillation, our approach is also good in preserving the identity, adhere more closely to the reference prompts and achieve the best 3D consistency. Although the Live3D + CLIP achieve the best ID_t score, the edited results are basically unchanged compared to the input. We suspect that Live3D does not have a latent space and loses the editing priors, making it challenging for the results of CLIP optimization to align well with prompts. Compared with PTI + CLIP methods, our model can enable precise alignment with input and prompts, while the baseline always generates low-fidelity textures, and the resulting geometry has many artifacts. In contrast to the 2D editing and subsequent 3D reconstruction pipeline (IP2P + Live3D), our system produces textures consistent with the prompt and aligns

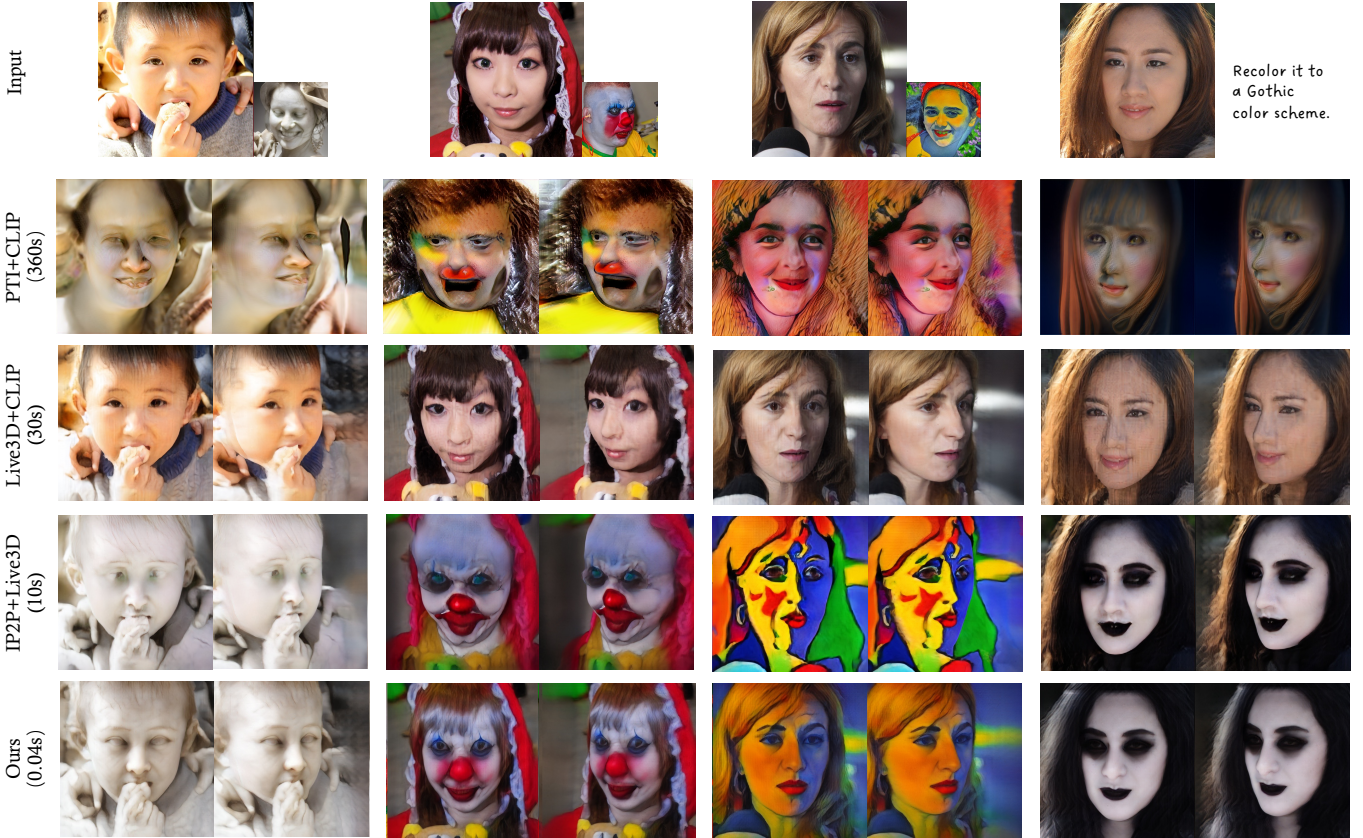


Fig. 4. **Qualitative comparisons.** We compare the results of several baselines with image prompts and text prompts. In each case, we include the edited portraits as well as their novel view renderings. Our method generates high-quality edited portraits with better 3D quality and alignment with the referenced prompts.



Fig. 5. **Novel prompt adaptation.** We show the intermediate testing results at 10s, 1min, 2min and 5min during adaptation with 10 paired training images.

better with the input structure. For example, as the second sample in Fig. 4 shows, our model can consistently retain the hair structure, while IP2P + Live3D cannot handle this. The third sample showcases that IP2P + Live3D introduces texture artifacts on the face and cannot inherit the style of prompts very well.

4.3 Adaptation to Customized Editing

With the trained editing network, our system already supports a variety of 3D-aware editing styles. To expand the selection and better conform to users' preferences, we offer an efficient method for fast adaptation to new prompts. Users can personalize the editing network by providing a modest set of 10 reference editing pairs. These pairs can be either handpicked from artist-created examples

or produced using text-guided image editing models. The adaptation process itself is remarkably fast, requiring only about 5 minutes to accomplish the learning of the novel prompts. In Fig. 5, we present the intermediate testing results in the adaptation process. Our model can quickly master the novel-prompt knowledge in about 2 minutes. With further training (e.g., 5 minutes), the edited results become more stylized, demonstrating a trade-off between the authenticity and the stylization. Upon completion of the adaptation, the system allows users to edit testing inputs in these newly learned styles with a minimal inference time of 0.04s. This rapid performance indicates that the system is well-optimized for real-time applications, providing a seamless and efficient user experience.

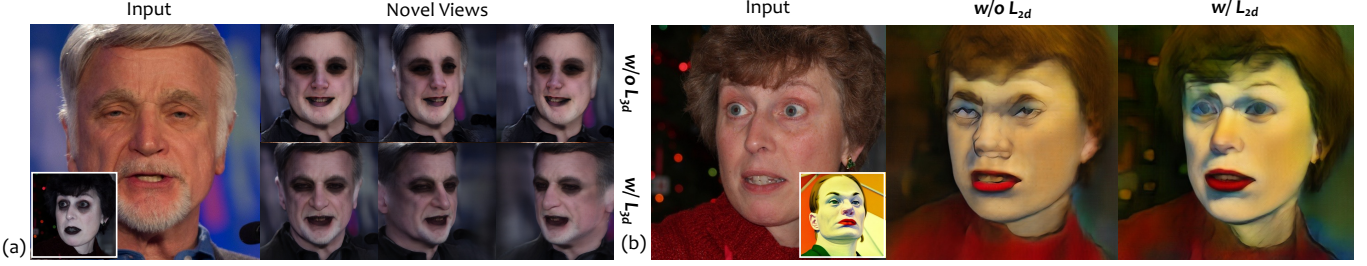


Fig. 6. Qualitative comparison for ablations on (a) the distillation loss of 3D GAN (\mathcal{L}_{3D}) and (b) diffusion models (\mathcal{L}_{2D}).

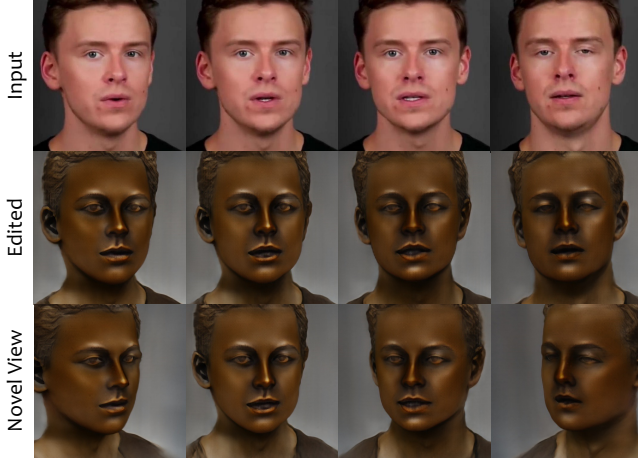


Fig. 7. Video editing results with 3DPE. We use text prompts "Bronze statue" to edit the input video. Our method can accurately reconstruct challenging facial expressions and achieve high-quality novel view renderings.

4.4 Ablation Studies

We analyze our model and validate our design choice by ablating the components.

\mathcal{L}_{3D} for Distillation of Live3D. We compare our model trained with and without \mathcal{L}_{3D} . As shown in Fig. 6, we observe that the model without \mathcal{L}_{3D} results in very flat geometry, and the synthesis of the side view loses the normal structure with many artifacts. This highlights the importance of the 3D knowledge from Live3D in training our model with 2D paired data, enabling the inference of reasonable face geometry without relying on any 3D data sources.

\mathcal{L}_{2D} for Distillation of Diffusion Models. We also study the effect of \mathcal{L}_{2D} . From Fig. 6, we observe that \mathcal{L}_{2D} is critical for our model, especially in preserving detailed texture. Without it, the edited image tends to lose appearance information from prompts and exhibits structural artifacts around the nose.

Ablation on Novel Prompt Adaptations. To investigate the ability of our method adapted to novel prompts, we conduct an ablation study on the number of novel-prompt data pairs required for training. We choose the golden statue as the novel prompt for demonstration and perform adaptation with 2, 5, 10, 20, or 50 pairs of novel-prompt data on a single A6000 GPU. We experimentally find that our model can converge in about 5 minutes, and therefore, we report the perceptual distance between the model output and the provided ground truth at 0.1min, 1min, 2min, and 5min for comparison. As shown in Tab. 2, our model can adapt to the new style in

Table 2. Ablation study on the number of data pairs used for novel prompt adaptation. We report LPIPS score after 0.1min, 1min, 2min, and 5min fine-tuning for evaluation.

#Pair/Time	0.1min	1min	2min	5min
2	0.6191	0.5431	0.5213	0.5212
5	0.6148	0.5324	0.5064	0.4971
10	0.6076	0.5242	0.4983	0.4935
20	0.5981	0.5525	0.4954	0.4895
50	0.5891	0.5718	0.4922	0.4797

around 2 minutes. As the number of provided data pairs increases, the model can adapt faster at the beginning.

4.5 Applications

One important application of our pipeline is to edit streaming videos, requiring accurate reconstruction and efficient editing simultaneously. We demonstrate the effectiveness of our pipeline on talking face videos, as illustrated in Fig. 7. Our method accurately reconstructs facial expressions, while achieving high-quality editing results. Since our method is 3D-aware, we can naturally view videos from novel perspectives. The demo video is available in the supplementary materials. To better experience our method, we design an interactive system that allows users for real-time editing, which is shown in Fig. 8. Users are required to provide a prompt to indicate the desired style, and an input image that is to be edited. By clicking the 'submit' button, the system will automatically apply our method on the given image and prompt, and output real-time edited image as well as novel-view edited results.

5 DISCUSSION

Limitations and Future work. Despite achieving state-of-the-art performance in terms of quality and efficiency, our system exhibits inconsistencies in the details for novel-view rendering. This occurs because the EG3D framework relies on a super-resolution module. Additionally, when our method is applied to video editing, it presents flickering artifacts since our model is designed for per-frame editing. Developing our methods for video editing could be an interesting avenue of future research.

Conclusion. We introduce 3DPE for real-time 3D-aware portrait editing. By distilling the powerful knowledge of diffusion models and 3D GANs into a lightweight module, our model significantly reduces editing time while ensuring quality. Additionally, our model supports fast adaptation to user-specified novel prompts. The advantages of our method empower us to generate photorealistic 3D portraits, a capability crucial for the visual effects industry, AR/VR systems, and teleconferencing, among other applications.

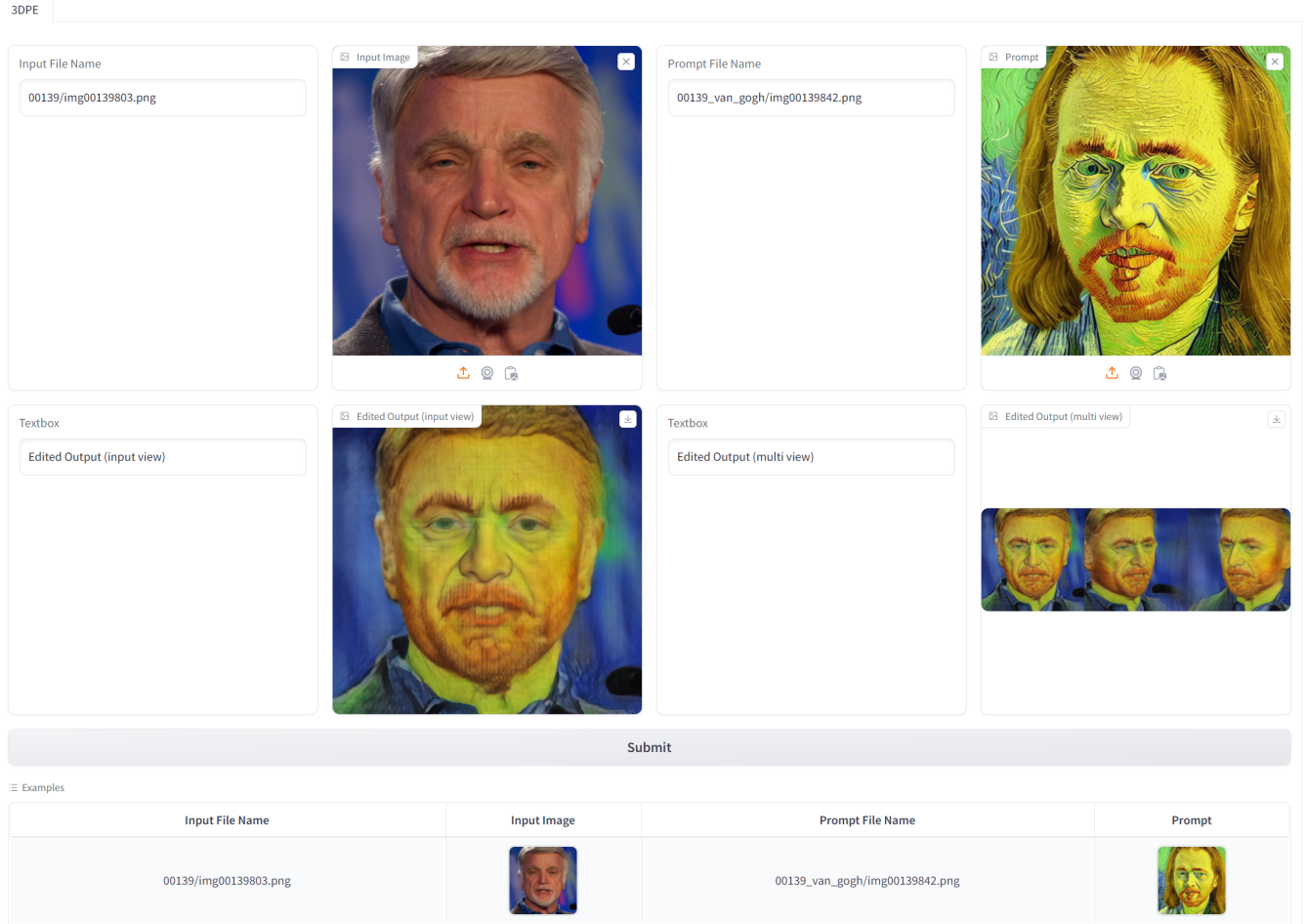


Fig. 8. **The interactive interface** that allows users to customize their editing.

REFERENCES

Rameen Abdal, Yipeng Qin, and Peter Wonka. 2019. Image2StyleGAN: How to Embed Images Into the StyleGAN Latent Space?. In *Int. Conf. Comput. Vis.*

Rameen Abdal, Yipeng Qin, and Peter Wonka. 2020. Image2StyleGAN++: How to Edit the Embedded Images?. In *IEEE Conf. Comput. Vis. Pattern Recog.*

Shivangi Aneja, Justus Thies, Angela Dai, and Matthias Nießner. 2023. Clipface: Text-guided editing of textured 3d morphable models. In *SIGGRAPH*.

Qingyan Bai, Yinghao Xu, Jiapeng Zhu, Weihao Xia, Yujiu Yang, and Yujun Shen. 2022. High-fidelity GAN inversion with padding space. In *Eur. Conf. Comput. Vis.*

Volker Blanz and Thomas Vetter. 2023. A morphable model for the synthesis of 3D faces. In *Seminal Graphics Papers: Pushing the Boundaries, Volume 2*.

Tim Brooks, Aleksander Holynski, and Alexei A Efros. 2023. Instructpix2pix: Learning to follow image editing instructions. In *IEEE Conf. Comput. Vis. Pattern Recog.*

Shengqu Cai, Anton Obukhov, Dengxin Dai, and Luc Van Gool. 2022. Pix2NeRF: Unsupervised Conditional p-GAN for Single Image to Neural Radiance Fields Translation. In *IEEE Conf. Comput. Vis. Pattern Recog.*

Mingdeng Cao, Xintao Wang, Zhongang Qi, Ying Shan, Xiaohu Qie, and Yingqiang Zheng. 2023. MasaCtrl: Tuning-Free Mutual Self-Attention Control for Consistent Image Synthesis and Editing. *arXiv preprint arXiv:2304.08465* (2023).

Duygu Ceylan, Chun-Hao P Huang, and Niloy J Mitra. 2023. Pix2video: Video editing using image diffusion. In *Proceedings of the IEEE/CVF International Conference on Computer Vision*. 23206–23217.

Wenhao Chai, Xun Guo, Gaoang Wang, and Yan Lu. 2023. Stablevideo: Text-driven consistency-aware diffusion video editing. In *Proceedings of the IEEE/CVF International Conference on Computer Vision*. 23040–23050.

Eric R Chan, Connor Z Lin, Matthew A Chan, Koki Nagano, Boxiao Pan, Shalini De Mello, Orazio Gallo, Leonidas J Guibas, Jonathan Tremblay, Sameh Khamis, et al. 2022. Efficient geometry-aware 3D generative adversarial networks. In *IEEE Conf. Comput. Vis. Pattern Recog.*

Eric R Chan, Marco Monteiro, Petr Kellnhofer, Jiajun Wu, and Gordon Wetzstein. 2021. pi-gan: Periodic implicit generative adversarial networks for 3d-aware image synthesis. In *IEEE Conf. Comput. Vis. Pattern Recog.*

Seunggyu Chang, Gihoon Kim, and Hayeon Kim. 2023. HairNeRF: Geometry-Aware Image Synthesis for Hairstyle Transfer. In *Int. Conf. Comput. Vis.*

Jiankang Deng, Jia Guo, Niannan Xue, and Stefanos Zafeiriou. 2019a. Arcface: Additive angular margin loss for deep face recognition. In *IEEE Conf. Comput. Vis. Pattern Recog.*

Yu Deng, Jiaolong Yang, Dong Chen, Fang Wen, and Xin Tong. 2020. Disentangled and controllable face image generation via 3d imitative-contrastive learning. In *IEEE Conf. Comput. Vis. Pattern Recog.*

Yu Deng, Jiaolong Yang, Sicheng Xu, Dong Chen, Yunde Jia, and Xin Tong. 2019b. Accurate 3d face reconstruction with weakly-supervised learning: From single image to image set. In *Proceedings of the IEEE/CVF conference on computer vision and pattern recognition workshops*.

Alexey Dosovitskiy, Lucas Beyer, Alexander Kolesnikov, Dirk Weissenborn, Xiaohua Zhai, Thomas Unterthiner, Mostafa Dehghani, Matthias Minderer, Georg Heigold, Sylvain Gelly, et al. 2020. An image is worth 16x16 words: Transformers for image recognition at scale. *arXiv preprint arXiv:2010.11929* (2020).

Chen Gao, Yichang Shih, Wei-Sheng Lai, Chia-Kai Liang, and Jia-Bin Huang. 2020. Portrait neural radiance fields from a single image. *arXiv preprint arXiv:2012.05903* (2020).

Michal Geyer, Omer Bar-Tal, Shai Bagon, and Tali Dekel. 2023. Tokenflow: Consistent diffusion features for consistent video editing. *arXiv preprint arXiv:2307.10373* (2023).

Alexandros Graikos, Nikolay Malkin, Nebojsa Jojic, and Dimitris Samaras. 2022. Diffusion models as plug-and-play priors. *Adv. Neural Inform. Process. Syst.* (2022).

Jiatao Gu, Lingjie Liu, Peng Wang, and Christian Theobalt. 2022. Stylenerf: A style-based 3d-aware generator for high-resolution image synthesis. In *Int. Conf. Learn. Represent.*

Jia Guo, Jinke Yu, Alexandros Lattas, and Jiankang Deng. 2022. Perspective reconstruction of human faces by joint mesh and landmark regression. In *Eur. Conf. Comput. Vis.*

Ayaan Haque, Matthew Tancik, Alexei A Efros, Aleksander Holynski, and Angjoo Kanazawa. 2023. Instruct-nerf2nerf: Editing 3d scenes with instructions. *arXiv preprint arXiv:2303.12789* (2023).

Erik Härkönen, Aaron Hertzmann, Jaakko Lehtinen, and Sylvain Paris. 2020. Ganspace: Discovering interpretable gan controls. *Adv. Neural Inform. Process. Syst.* (2020).

Kaiming He, Xinlei Chen, Saining Xie, Yanghao Li, Piotr Dollár, and Ross Girshick. 2022. Masked autoencoders are scalable vision learners. In *IEEE Conf. Comput. Vis. Pattern Recog.*

Amir Hertz, Kfir Aberman, and Daniel Cohen-Or. 2023. Delta denoising score. In *Int. Conf. Comput. Vis.*

Edward J Hu, Yelong Shen, Phillip Wallis, Zeyuan Allen-Zhu, Yuanzhi Li, Shean Wang, Lu Wang, and Weizhu Chen. 2021. Lora: Low-rank adaptation of large language models. *arXiv preprint arXiv:2106.09685* (2021).

Junha Hyung, Sungwon Hwang, Daejin Kim, Hyunji Lee, and Jaegul Choo. 2023. Local 3D Editing via 3D Distillation of CLIP Knowledge. In *IEEE Conf. Comput. Vis. Pattern Recog.*

Kaiwen Jiang, Shu-Yu Chen, Hongbo Fu, and Lin Gao. 2023. NeRFFaceLighting: Implicit and Disentangled Face Lighting Representation Leveraging Generative Prior in Neural Radiance Fields. *ACM Trans. Graph.* (2023).

Tero Karras, Samuli Laine, and Timo Aila. 2019. A style-based generator architecture for generative adversarial networks. In *IEEE Conf. Comput. Vis. Pattern Recog.*

Jaehoon Ko, Kyusun Cho, Daewon Choi, Kwangrok Ryoo, and Seungryong Kim. 2023. 3d gan inversion with pose optimization. In *IEEE Winter Conf. Appl. Comput. Vis.*

Nupur Kumari, Bingliang Zhang, Richard Zhang, Eli Shechtman, and Jun-Yan Zhu. 2023. Multi-concept customization of text-to-image diffusion. In *Proceedings of the IEEE/CVF Conference on Computer Vision and Pattern Recognition*. 1931–1941.

Junnan Li, Dongxu Li, Caiming Xiong, and Steven Hoi. 2022. Blip: Bootstrapping language-image pre-training for unified vision-language understanding and generation. In *Int. Conf. Mach. Learn.*

Jianhui Li, Jianmin Li, Haqij Zhang, Shilong Liu, Zhengyi Wang, Zihao Xiao, Kaiwen Zheng, and Jun Zhu. 2023a. PREIM3D: 3D Consistent Precise Image Attribute Editing from a Single Image. In *IEEE Conf. Comput. Vis. Pattern Recog.*

Jianhui Li, Shilong Liu, Zidong Liu, Yikai Wang, Kaiwen Zheng, Jinghui Xu, Jianmin Li, and Jun Zhu. 2023b. InstructPix2NeRF: Instructed 3D Portrait Editing from a Single Image. *arXiv preprint arXiv:2311.02826* (2023).

Connor Z Lin, David B Lindell, Eric R Chan, and Gordon Wetzstein. 2022. 3d gan inversion for controllable portrait image animation. *arXiv preprint arXiv:2203.13441* (2022).

Shaoteng Liu, Yuechen Zhang, Wenbo Li, Zhe Lin, and Jiaya Jia. 2023b. Video-p2p: Video editing with cross-attention control. *arXiv preprint arXiv:2303.04761* (2023).

Zhiheng Liu, Ruili Feng, Kai Zhu, Yifei Zhang, Kecheng Zheng, Yu Liu, Deli Zhao, Jingren Zhou, and Yang Cao. 2023a. Cones: Concept neurons in diffusion models for customized generation. *arXiv preprint arXiv:2303.05125* (2023).

Chenlin Meng, Yutong He, Yang Song, Jiameng Song, Jiajun Wu, Jun-Yan Zhu, and Stefano Ermon. 2021. Sdedit: Guided image synthesis and editing with stochastic differential equations. *arXiv preprint arXiv:2108.01073* (2021).

Roy Or-El, Xuan Luo, Mengyi Shan, Eli Shechtman, Jeong Joon Park, and Ira Kemelmacher-Shlizerman. 2022. Stylesdf: High-resolution 3d-consistent image and geometry generation. In *IEEE Conf. Comput. Vis. Pattern Recog.*

Hao Ouyang, Qiuyu Wang, Yuxi Xiao, Qingyan Bai, Juntao Zhang, Kecheng Zheng, Xiaowei Zhou, Qifeng Chen, and Yujun Shen. 2023. Codef: Content deformation fields for temporally consistent video processing. *arXiv preprint arXiv:2308.07926* (2023).

Xingang Pan, Xudong Xu, Chen Change Loy, Christian Theobalt, and Bo Dai. 2021. A shading-guided generative implicit model for shape-accurate 3d-aware image synthesis. *Adv. Neural Inform. Process. Syst.* (2021).

Pascal Payan, Reinhard Knothe, Brian Amberg, Sami Romdhani, and Thomas Vetter. 2009. A 3D face model for pose and illumination invariant face recognition. In *IEEE international conference on advanced video and signal based surveillance*.

Ben Poole, Ajay Jain, Jonathan T Barron, and Ben Mildenhall. 2022. Dreamfusion: Text-to-3d using 2d diffusion. *arXiv preprint arXiv:2209.14988* (2022).

Chenyang Qi, Xiaodong Cun, Yong Zhang, Chenyang Lei, Xintao Wang, Ying Shan, and Qifeng Chen. 2023. Fatezero: Fusing attentions for zero-shot text-based video editing. *arXiv preprint arXiv:2303.09535* (2023).

Alec Radford, Jong Wook Kim, Chris Hallacy, Aditya Ramesh, Gabriel Goh, Sandhini Agarwal, Girish Sastry, Amanda Askell, Pamela Mishkin, Jack Clark, et al. 2021. Learning transferable visual models from natural language supervision. In *Int. Conf. Mach. Learn.*

Daniel Roich, Ron Mokady, Amit H Bermano, and Daniel Cohen-Or. 2022. Pivotal tuning for latent-based editing of real images. *ACM Trans. Graph.* (2022).

Robin Rombach, Andreas Blattmann, Dominik Lorenz, Patrick Esser, and Björn Ommer. 2022. High-resolution image synthesis with latent diffusion models. In *IEEE Conf. Comput. Vis. Pattern Recog.*

Nataniel Ruiz, Yuanzhen Li, Varun Jampani, Yael Pritch, Michael Rubinstein, and Kfir Aberman. 2023. Dreambooth: Fine tuning text-to-image diffusion models for subject-driven generation. In *IEEE Conf. Comput. Vis. Pattern Recog.*

Katja Schwarz, Yiyi Liao, Michael Niemeyer, and Andreas Geiger. 2020. Graf: Generative radiance fields for 3d-aware image synthesis. In *Adv. Neural Inform. Process. Syst.*

Katja Schwarz, Axel Sauer, Michael Niemeyer, Yiyi Liao, and Andreas Geiger. 2022. Voxgraf: Fast 3d-aware image synthesis with sparse voxel grids. *Adv. Neural Inform. Process. Syst.* (2022).

Yujun Shen, Jinjin Gu, Xiaou Tang, and Bolei Zhou. 2020a. Interpreting the latent space of GANs for semantic face editing. In *IEEE Conf. Comput. Vis. Pattern Recog.*

Yujun Shen, Ceyuan Yang, Xiaou Tang, and Bolei Zhou. 2020b. InterFaceGAN: Interpreting the Disentangled Face Representation Learned by GANs. *IEEE Trans. Pattern Anal. Mach. Intell.* (2020).

Zifan Shi, Sida Peng, Yinghao Xu, Andreas Geiger, Yiyi Liao, and Yujun Shen. 2022a. Deep generative models on 3d representations: A survey. *arXiv preprint arXiv:2210.15663* (2022).

Zifan Shi, Yujun Shen, Yinghao Xu, Sida Peng, Yiyi Liao, Sheng Guo, Qifeng Chen, and Dit-Yan Yeung. 2023. Learning 3d-aware image synthesis with unknown pose distribution. In *IEEE Conf. Comput. Vis. Pattern Recog.*

Zifan Shi, Yinghao Xu, Yujun Shen, Deli Zhao, Qifeng Chen, and Dit-Yan Yeung. 2022b. Improving 3d-aware image synthesis with a geometry-aware discriminator. *Adv. Neural Inform. Process. Syst.* (2022).

Ivan Skorokhodov, Sergey Tulyakov, Yiqun Wang, and Peter Wonka. 2022. Epigraf: Rethinking training of 3d gans. In *Adv. Neural Inform. Process. Syst.*

Jingxiang Sun, Xuan Wang, Yichun Shi, Lizhen Wang, Jue Wang, and Yebin Liu. 2022a. Ide-3d: Interactive disentangled editing for high-resolution 3d-aware portrait synthesis. *ACM Trans. Graph.* (2022).

Jingxiang Sun, Xuan Wang, Yong Zhang, Xiaoyu Li, Qi Zhang, Yebin Liu, and Jue Wang. 2022b. Fenerf: Face editing in neural radiance fields. In *IEEE Conf. Comput. Vis. Pattern Recog.*

Alex Tretiwhick, Matthew Chan, Michael Stengel, Eric Chan, Chao Liu, Zhiding Yu, Sameh Khamis, Manmohan Chandraker, Ravi Ramamoorthi, and Koki Nagano. 2023. Real-time radiance fields for single-image portrait view synthesis. *ACM Trans. Graph.* (2023).

Qiyu Wang, Zifan Shi, Kecheng Zheng, Yinghao Xu, Sida Peng, and Yujun Shen. 2023b. Benchmarking and Analyzing 3D-aware Image Synthesis with a Modularized Codebase. *arXiv preprint arXiv:2306.12423* (2023).

Wen Wang, Yan Jiang, Kangyang Xie, Zide Liu, Hao Chen, Yue Cao, Xinlong Wang, and Chunhua Shen. 2023a. Zero-shot video editing using off-the-shelf image diffusion models. *arXiv preprint arXiv:2303.17599* (2023).

Youjia Wang, Teng Xu, Yiwen Wu, Minzhang Li, Wenzheng Chen, Lan Xu, and Jingyi Yu. 2022. NARRATE: A Normal Assisted Free-View Portrait Stylizer. *arXiv preprint arXiv:2207.00974* (2022).

Weihao Xia and Jing-Hao Xue. 2023. A Survey on Deep Generative 3D-aware Image Synthesis. *Comput. Surveys* (2023).

Jiaxin Xie, Hao Ouyang, Jingtian Piao, Chenyang Lei, and Qifeng Chen. 2023. High-fidelity 3D GAN Inversion by Pseudo-multi-view Optimization. In *IEEE Conf. Comput. Vis. Pattern Recog.*

Yinghao Xu, Sida Peng, Ceyuan Yang, Yujun Shen, and Bolei Zhou. 2022. 3D-aware Image Synthesis via Learning Structural and Textural Representations. In *IEEE Conf. Comput. Vis. Pattern Recog.*

Yinghao Xu, Yujun Shen, Jiapeng Zhu, Ceyuan Yang, and Bolei Zhou. 2021. Generative hierarchical features from synthesizing images. In *IEEE Conf. Comput. Vis. Pattern Recog.*

Shuai Yang, Yifan Zhou, Ziwei Liu, and Chen Change Loy. 2023. Rerender A Video: Zero-Shot Text-Guided Video-to-Video Translation. *arXiv preprint arXiv:2306.07954* (2023).

Fei Yin, Yong Zhang, Xuan Wang, Tengfei Wang, Xiaoyu Li, Yuan Gong, Yanbo Fan, Xiaodong Cun, Ying Shan, Cengiz Oztireli, et al. 2023. 3d gan inversion with facial symmetry prior. In *IEEE Conf. Comput. Vis. Pattern Recog.*

Lvmin Zhang, Anyi Rao, and Maneesh Agrawala. 2023. Adding conditional control to text-to-image diffusion models. In *Int. Conf. Comput. Vis.*

Richard Zhang, Phillip Isola, Alexei A Efros, Eli Shechtman, and Oliver Wang. 2018. The unreasonable effectiveness of deep features as a perceptual metric. In *IEEE Conf. Comput. Vis. Pattern Recog.*

Jiapeng Zhu, Yujun Shen, Deli Zhao, and Bolei Zhou. 2020. In-domain GAN inversion for real image editing. In *Eur. Conf. Comput. Vis.*

Jun-Yan Zhu, Philipp Krähenbühl, Eli Shechtman, and Alexei A Efros. 2016. Generative visual manipulation on the natural image manifold. In *Eur. Conf. Comput. Vis.*

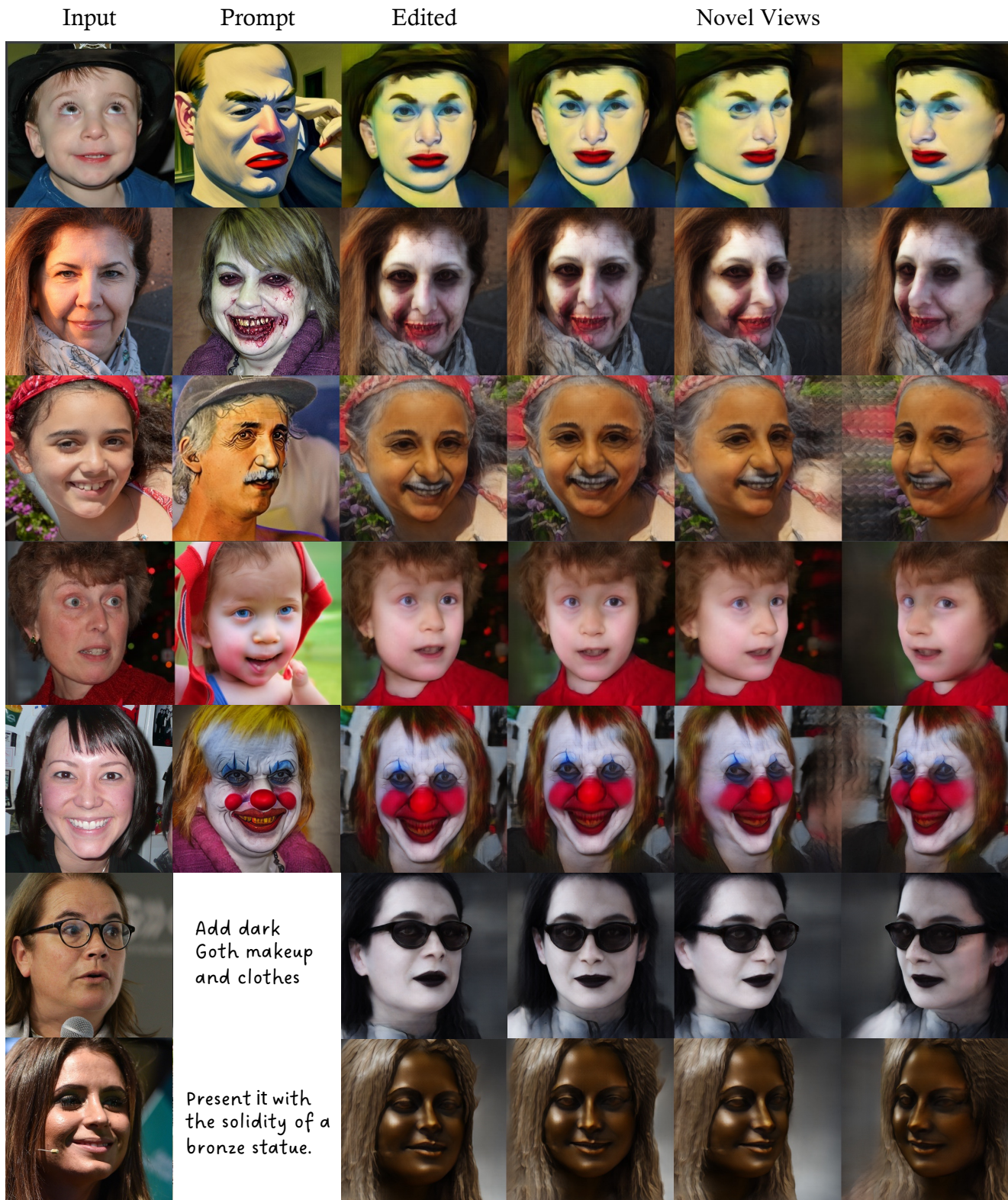


Fig. 9. Additional qualitative results.